

*Letter to the Editor***Physical conditions in the partially ionized zone of the Orion nebula***César Esteban¹, Manuel Peimbert², and Silvia Torres-Peimbert²¹ Instituto de Astrofísica de Canarias, E-38200 La Laguna, Tenerife, Canary Islands, Spain (cel@ll.iac.es)² Instituto de Astronomía, UNAM Apdo. Postal 70-264, Mexico D.F. 04510, Mexico (peimbert@astroscu.unam.mx, silvia@astroscu.unam.mx)

Received 30 November 1998 / Accepted 21 December 1998

Abstract. We report the first reliable measurement of the nebular [O I] $\lambda 5577$ emission line in the Orion nebula. Diagnostic diagrams based on the [O I] $\lambda\lambda 5577, 6300$, and [N I] $\lambda\lambda 3467, 5198, 5200$ emission lines indicate that the bulk of the nebular emission in the partially ionized zone of the Orion nebula is produced in regions with low to moderate electron densities ($2 \times 10^3 - 4 \times 10^4 \text{ cm}^{-3}$) and with electron temperatures in the 8900 to 12400 K range. This result implies that models based on emission originating in high-density partially ionized zones are not applicable to explain the observed [Fe II] spectrum in the optical region.

Key words: ISM: H II regions – ISM: individual objects: Orion nebula – ISM: structure

1. Introduction

The Orion nebula is the brightest and most studied Galactic H II region. Its structure, motions and chemical abundances are known with considerably high detail (e.g. O'Dell 1994; Wen & O'Dell 1995; Osterbrock, Tran, & Veilleux 1992; Esteban et al. 1998, hereafter EPTE).

Recently, Bautista, Pradhan, & Osterbrock (1994) reported the presence of high density regions in the Orion nebula, $N_e \approx 10^5 - 10^7 \text{ cm}^{-3}$, based on diagnostic diagrams using [Fe II] emission lines. In addition, these authors found that the Fe⁺ abundances derived from different [Fe II] lines measured by Osterbrock et al. (1992) present a lower dispersion when high electron densities are considered. Bautista et al. (1994) argued also that the [Fe II] emission is probably produced in the partially ionized zone (PIZ) and that these high density zones are the denser parts of the ionization front at the edge of the H II region.

The ideas related to the PIZ and to the mechanisms responsible for the excitation of the [Fe II] lines were developed further in a series of papers by Bautista & Pradhan (1995), Bautista, Peng & Pradhan (1996) and Bautista & Pradhan (1998, here-

after BP). BP present a new model with a fully ionized H II region, FIZ, with densities of the order of a few 10^3 cm^{-3} and a dynamic partially ionized H II/H I region, PIZ, at densities of $10^5 - 10^7 \text{ cm}^{-3}$. In this model the [Fe II] lines originate in both zones the FIZ and the PIZ; while most of the emission of the IR lines originates in the FIZ, most of the emission of the optical lines originates in the PIZ. From this model and based on the [Fe II] lines they find that the Fe/O ratio is between 1/2 and 1/3 solar. By assuming that all the [Fe II] emission is produced in the FIZ they find that the Fe/O ratio is between 1/4 and 1/2 solar

On the other hand, Lucy (1995) finds an alternative explanation for the observed [Fe II] spectrum of the Orion nebula, which is based on the presence of important fluorescence effects on the optical [Fe II] lines. Baldwin et al. (1996) found consistent results with Lucy, reproducing the [Fe II] spectrum in a low density medium considering collisional excitation for the IR lines and fluorescence for the optical ones. Moreover, Rodríguez (1996, 1998) analysed a large number of [Fe II] lines in seven bright galactic H II regions, finding that the observed properties of the [Fe II] spectrum are more consistent with the presence of fluorescence effects, she concludes that the bulk of the [Fe II] emission in the Orion nebula originates in regions with densities of a few 10^3 cm^{-3} and that the abundances derived from the [Fe II] lines are unreliable.

To try to solve this controversy we decided to take a different approach: to determine the physical conditions of the PIZ based on the emission lines of [O I] and [N I]. In this letter we present the first detection in the Orion nebula of the [O I] $\lambda 5577$ line, the [O I] $I(5577)/I(6300+6363)$ ratio, a measurement of the [N I] $I(5198)/I(5200)$ ratio, and an upper limit for the [N I] $I(3467)/I(5198+5200)$ ratio; we will also discuss the implications of these line ratios for the study of the mechanisms of excitation of the [Fe II] lines. Osterbrock et al. (1992) presented a detection of the $\lambda 5577$ line which yielded an $I(6300+6363)/I(5577)$ value of 22; however in a subsequent paper Baldwin et al. (1996) obtained a lower limit for $I(6300 + 6363)/I(5577)$ of 71 from spectroscopic data taken with the Cassegrain echelle spectrograph on the 4 m telescope at CTIO and 29 from spectra taken with the Faint Object Spectrograph on the *Hubble Space Telescope (HST)*; Baldwin et al. (1996) conclude that the [O I] lines presented by Osterbrock et

Send offprint requests to: César Esteban

* Based on data obtained at the Observatorio Astronómico Nacional, SPM, B.C., México

al. (1992) were severely affected by sky emission and therefore useless for plasma diagnostics.

2. The data

We have reanalyzed the echelle spectra published previously by EPTE and have detected the nebular [O I] $\lambda 5577$ line. We have also determined an upper limit for the [N I] $\lambda\lambda 3466.51 + 3466.54$ lines, hereafter the $\lambda 3467$ line.

The observations were carried out with the 2.1-m telescope of the Observatorio Astronómico Nacional at San Pedro Mártir, Baja California, Mexico, on 1995 March 25 and 26. The high resolution spectra were obtained using the REOSC Echelle Spectrograph. This instrument gives a resolution of $0.234 \text{ \AA pixel}^{-1}$ at $H\alpha$ using a Tektronic CCD chip of 1024×1024 pixels with a $24 \mu\text{m}^2$ pixels size. The spectral resolution is of 0.5 \AA FWHM and the accuracy in the wavelength determination of emission lines is about $1\text{-}1.5 \text{ km s}^{-1}$.

The observations correspond to slits covering $26.6 \times 2 \text{ arcsec}^2$ in the red and $13.3 \times 2 \text{ arcsec}^2$ in the blue exposures, both slits were oriented in the east-west direction and located at 25 arcsec south and 10 arcsec west of θ^1 Orionis C (position 2 of EPTE). The red spectra cover from $\lambda\lambda 4500$ to 6850 in 17 spectral orders; and the blue spectra cover from $\lambda\lambda 3300$ to 5800 in 26 spectral orders. A detailed description of the observations and data reduction can be found in EPTE. EPTE do not report the intensities of the lines in the $\lambda\lambda 3300$ to 3550 range due to their relatively low signal to noise ratio and partial overlapping between spectral orders, nevertheless due to the importance of the [N I] $\lambda 3467$ line, we reanalyzed our data and present an upper limit for the intensity of this line in Table 1.

These observations represent a clear improvement with respect to the ones obtained by Baldwin et al. (1996). Firstly, the exposure time of the *HST* spectra (225 s) obtained by these authors is substantially shorter than the one-hour spectrum obtained by EPTE. Secondly, although Baldwin et al. (1996) do not indicate the exposure time of their 4m CTIO data (of similar spectral resolution), the comparison of their spectrum (see their Fig. 1) and our data (Fig. 1 of this letter) indicates the larger signal-to-noise ratio of the spectrum taken at San Pedro Mártir.

3. The physical conditions in the PIZ

The profiles of the three [O I] lines observed in our deep red spectrum are shown in Fig. 1, all these profiles show clear linesplitting. A double Gaussian profile fit procedure was applied to obtain the observational parameters of each component (central wavelength and line intensity). The Gaussian fitting procedure was performed making use of the Starlink DIPSO software package (Howarth & Murray 1990) and the graphical results of the fitting are shown also in Fig. 1. In Table 1 we include the observed (relative to the heliocentric reference frame) and laboratory wavelengths of each component of the [O I] and [N I] lines, and the heliocentric velocity and the dereddened line intensity ratios (relative to $H\beta$) of the nebular component. The adopted reddening coefficient, $C(H\beta)$, for this slit position is

Table 1. Observational parameters of the [O I] and [N I] lines

Ion	λ_{lab} (\AA)	λ_{obs} (\AA)	Comp.	V_{hel} (km s^{-1})	$I(\lambda)/I(H\beta)$
[O I]	5577.34	5577.34	Sky
		5577.80	Neb.	+24.6	0.000117
	6300.30	6300.31	Sky
		6300.79	Neb.	+23.3	0.00806
[N I]	6363.78	6363.78	Sky
		6364.33	Neb.	+25.9	0.00238
	3467	...	Neb.	...	<0.001
	5197.90	5198.37	Neb.	+27.1	0.00160
	5200.26	5200.72	Neb.	+26.5	0.00096

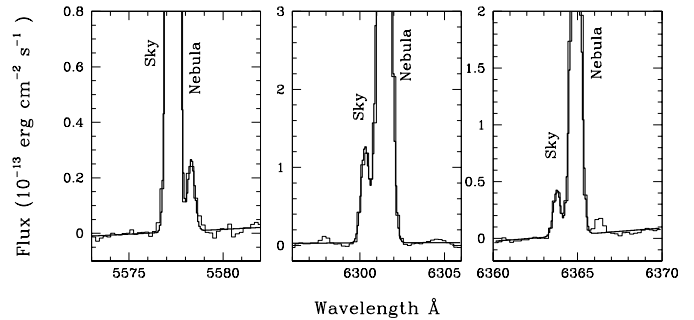


Fig. 1. Examples of double Gaussian fit to the three [O I] emission lines observed. The identification of each component as corresponding to sky or nebular emission is indicated.

0.39 ± 0.04 and was derived previously by EPTE. As it can be seen in Table 1, the heliocentric velocity of the redshifted component of the [O I] $\lambda 5577$ line is consistent (within the estimated uncertainty of about 1.2 km s^{-1}) with the velocities of the redshifted components of the other much brighter [O I] lines. The average heliocentric velocity of the bright nebular components is $24.6 \pm 1.8 \text{ km s}^{-1}$, in agreement with $26.8 \pm 1.4 \text{ km s}^{-1}$, the average velocity found for the two [N I] lines observed in the same set of data (also included in Table 1), and with the value of 26.7 km s^{-1} obtained by O'Dell & Wen (1992) for the nebular [O I] emission in the same zone. Moreover, the heliocentric radial velocity of the molecules in OMC 1 (the molecular cloud associated to the Orion nebula) is close to 27 km s^{-1} (Goudis 1982). All these observational facts indicate undoubtedly that the redshifted component of the [O I] $\lambda 5577$ line is truly nebular and should arise in the transition zone of the nebula, as it was stated by O'Dell & Wen (1992).

In Fig. 2 we present a T_e versus N_e diagram based on the [N I] and [O I] line ratios presented in Table 1. The T_e and N_e values for the different line ratios have been computed using the five-level program for the analysis of emission-line nebulae of Shaw & Dufour (1995) together with the atomic data compiled by Pradhan & Peng (1995). The $I(6300 + 6363)/I(5577)$ ratio provides us with a relationship between N_e and T_e , therefore we need at least another observational constraint to determine N_e and T_e . The [N I] $I(5198)/I(5200)$ ratio is close to N_e saturation limit and can not provide us with an upper limit for N_e , but

Table 2. Properties of the Orion nebula: models and observations

	Model		Observations ^{3,4,5}	Observations ^{3,4,6}
	BFM ¹	RSHE ²		
O/H	3.81×10^{-4}	4.0×10^{-4}	4.37×10^{-4}	
N/H	8.7×10^{-5}	6.8×10^{-5}	6.03×10^{-5}	
N/O	0.228	0.170	0.138	
O ⁰ /O	3.46×10^{-3}	1.74×10^{-2}	3.30×10^{-3}	4.90×10^{-3}
N ⁰ /N	7.81×10^{-4}	2.09×10^{-2}	$(0.86 - 2.79) \times 10^{-2}$	$(0.61 - 3.5) \times 10^{-2}$
N ⁰ /O ⁰	0.052	0.204	0.36 - 1.17	0.17 - 0.99
O ⁰ /H ⁺	1.31×10^{-6}	6.96×10^{-6}	1.44×10^{-6}	2.12×10^{-6}
N ⁰ /H ⁺	6.79×10^{-8}	1.42×10^{-6}	$(0.52 - 1.68) \times 10^{-6}$	$(0.37 - 2.1) \times 10^{-6}$
$N_e(N^0, O^0)$ (cm ⁻³)	≈6000	≈4000
$T_e([O\ I])$ (K)	9900	≈7500	10400^{+2000}_{-1100}	10000^{+1800}_{-1100}
$N_e([N\ I] 5198/5200)$ (cm ⁻³)	>2000	>4350
$N_e([N\ I] 3467)$ (cm ⁻³)	<38000	<35800
$N_e([S\ II])$ (cm ⁻³)	6410^{+3010}_{-2900}	

¹ Baldwin et al. (1991); ² Rubin et al. (1991); ³ Esteban et al. (1998); ⁴ This paper; ⁵ Mendoza (1983);

⁶ Pradhan & Peng (1995)

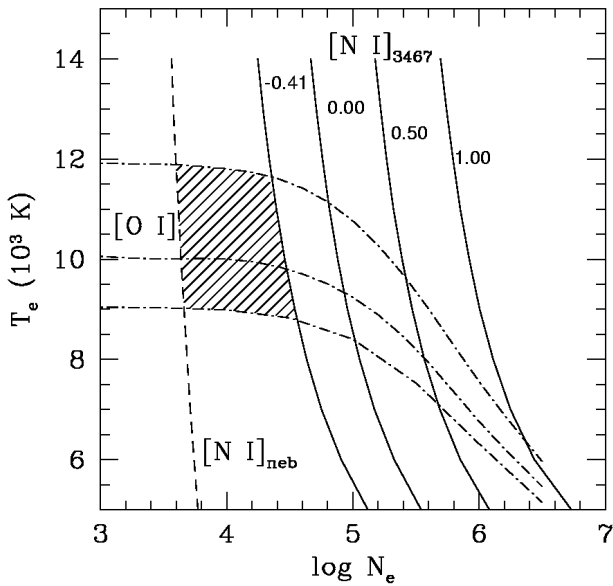


Fig. 2. Temperature (K) vs. density (cm⁻³) diagram for the PIZ in the direction of position 2. The vertical dashed line corresponds to the minimum density allowed by the [N I] $I(5198)/I(5200)$ ratio. The three dot-dashed lines correspond to the 60, 89 and 118 [O I] $I(6300+6363)/I(5577)$ ratios. The four solid lines correspond to the maximum density allowed by different [N I] $I(3467)/I(5198+5200)$ line ratios; the numbers inside the figure denote $\log I(3467)/I(5198+5200)$ values, -0.41 dex corresponds to the determined upper limit for position 2 in this paper. The permitted T_e and N_e values are represented by the shaded area.

gives us the lower limit for N_e presented in Fig. 2, where we have adopted a lower limit of 1.39 for the [N I] $I(5198)/I(5200)$ ratio. Fortunately, we can use the $I(3467)/I(5198+5200)$ ratio to obtain an upper limit for N_e , the computed upper limit for this line ratio is -0.41 dex and is also presented in Fig. 2. In this figure we also present a shadow area that corresponds to

the permitted region by the three observational constraints, this region gives N_e in the range $2 \times 10^3 - 4 \times 10^4$ cm⁻³ and T_e : 9000-12000 K.

It is also possible to determine an upper limit for the [N I] $\lambda 3467$ line intensity from the data presented by Osterbrock et al. (1992). The He I $\lambda 3479$ line was detected with an intensity of 0.000695 relative to H β . By adopting an upper limit for $I(3467)/I(H\beta)$ of 0.0007, the $I(5198+5200)/I(H\beta)$ value reported by Osterbrock. et al., and a $T_e = 10000$ we find that $N_e < 3 \times 10^4$ cm⁻³, in agreement with our estimations above. Kaler, Aller & Bowen (1965) did not detect the $\lambda 3467$ line either and a similar upper limit for N_e can be derived from their observations.

From the atomic data compilation by Mendoza (1983) a similar figure to Fig. 2 can be obtained. Note that the rate coefficients for electron impact presented by Mendoza for N I and O I are the same as those presented by Pradhan & Peng (1995), while the radiative transition probabilities presented by Mendoza are more recent than those presented by Pradhan & Peng. In Table 2 we present some abundance ratios and physical parameters derived from the atomic data sets compiled by both groups of authors.

In Table 2 we also present some characteristics of the models by Baldwin et al. (1991, hereafter BFM) and Rubin et al. (1991, hereafter RSHE), together with properties derived from observed line ratios. BFM presents properties averaged over radius, while RSHE properties averaged over the entire volume of the H II region; in these models the O/H, N/H and $N_e(H^+)$ values are assumed to match observed line intensities, while the O⁰/H⁺, N⁰/H⁺, $N_e(N^0, O^0)$ and T_e values are predicted by the models.

We define $N_e(N^0, O^0)$ and $T_e([O\ I])$ as the values derived from the forbidden line intensities predicted by the models. Unfortunately BFM and RSHE do not present explicitly the values of $N_e(N^0, O^0)$ and $T_e([O\ I])$ but they can be estimated from the

figures and tables given by them. In the partially ionized zone T_e varies from a maximum value given by $T_e([\text{O II}])$ to practically zero. The average temperature in the O I zone, 6215 K, given by RSHE is a lower limit to $T_e([\text{O I}])$ because the temperature dependence of the emission lines is not included in their determination. The $T_e([\text{O I}])$ value for the BFM model was derived from the $[\text{O I}] I(5577)/I(6300)$ ratio predicted by Baldwin et al. (1996) for Model A and the atomic data compiled by Mendoza (1983).

The observed O^0/O , $T_e([\text{O I}])$, and O^0/H^+ values are in excellent agreement with the values predicted by the BFM model. On the other hand, the N^0/O^0 observed value is in good agreement with the RSHE one and considerably higher than the BFM value. Note that if N_e were higher than $4 \times 10^4 \text{ cm}^{-3}$ the N^0/O^0 value derived from observations would become even higher than the maximum values presented in Table 2, increasing the discrepancy between the models and the observations.

From photoionization models and partially due to the ionization potentials of O I (13.6 eV), N I (14.5 eV), Fe II (16.2 eV), and S II (23.3 eV), the [O I] and [N I] lines are expected to originate farther away from the ionizing stars than the [Fe II] lines, and even farther than the [S II] lines. Therefore, the average density where the [Fe II] lines originate should be intermediate between those derived from the [N I] lines and the [S II] lines, which according to Table 2 is considerably smaller than the density derived by BP from the [Fe II] lines under the assumption that fluorescence effects are negligible. To obtain $N_e = 10^6 \text{ cm}^{-3}$ the [N I] $\lambda 3467$ line has to be at least an order of magnitude brighter than the upper limit presented in Table 1 (see Fig. 2).

4. Summary

In this *Letter*, we report the first reliable detection of the nebular [O I] $\lambda 5577$ line in the Orion nebula. Based on [O I] and [N I] line ratios we have found that these lines originate in the PIZ with $2000 < N_e(\text{PIZ}) < 40000 \text{ cm}^{-3}$ and $8900 < T_e(\text{PIZ}) < 12400 \text{ K}$. From photoionization models it follows that the $N_e(\text{Fe II})$ value should be intermediate between that given by $N_e(\text{PIZ})$ and $N_e(\text{S II})$ and consequently that $2000 < N_e(\text{Fe II})(\text{PIZ}) < 40000 \text{ cm}^{-3}$. These low densities probably indicate that fluorescence effects are important in the excitation of [Fe II]

lines in the optical region. Consequently the Fe/O abundances derived from the Fe^+/O^0 ratios under the assumptions that fluorescence effects for the [Fe II] lines are negligible and that $N_e(\text{Fe II}) \sim 10^6 \text{ cm}^{-3}$ are unreliable.

Acknowledgements. It is a pleasure to acknowledge several fruitful discussions with M. Rodríguez. We are grateful to the referee, L. Lucy, for his useful suggestions. CE would like to thank all the members of the Instituto de Astronomía, UNAM, for their warm hospitality during his stays in Mexico. This research was partially funded through grant no. PB94-1108 from the Dirección General de Investigación Científica y Técnica of the Spanish Ministerio de Educación y Ciencia and grants DGAPA-UNAM IN109696 and CONACyT 25451-E (Mexico).

References

- Baldwin, J. A. et al. 1996, *ApJ*, 468, L115
 Baldwin, J. A., Ferland, G. J., Martin, P. G., Corbin, M. R., Cota, S. A., Peterson, B. M., Slettebak, A., 1991, *ApJ*, 374, 580 (BFM)
 Bautista, M. A., Pradhan, A. K., 1995, *ApJ*, 442, L68
 Bautista, M. A., Pradhan, A. K., 1998, *ApJ*, 492, 650 (BP)
 Bautista, M. A., Peng, J., Pradhan, A. K., 1996, *ApJ*, 460, 372
 Bautista, M. A., Pradhan, A. K., Osterbrock D. E., 1994, *ApJ*, 432, L135
 Esteban, C., Peimbert, M., Torres-Peimbert, S., Escalante, V., 1998, *MNRAS*, 295, 401 (EPTE)
 Howarth, I. D., Murray, J., 1990, SERC Starlink User Note No. 50
 Goudis, C., 1982, *The Orion Complex: A Case Study of Interstellar Matter* (Dordrecht: Reidel)
 Kaler, J. B., Aller, L. H., Bowen, I. S., 1965, *ApJ*, 141, 912
 Lucy, L. B., 1995, *A&A*, 294, 555
 Mendoza, C., 1983, *IAU Symp. 103, Planetary Nebulae*, Flower D.R. (ed.), Dordrecht, Kluwer, 143
 O'Dell, C. R., 1994, *Ap&SS*, 216, 267
 O'Dell, C. R., Wen, Z., 1992, *ApJ*, 387, 229
 Osterbrock, D. E., Tran, H. D., Veilleux, S., 1992, *ApJ*, 389, 305
 Pradhan, A. K., & Peng, J., 1995, *The Analysis of Emission Lines*, Williams R. E., Livio M. (eds.), Cambridge University Press, p. 8
 Rodríguez, M., 1996, *A&A*, 313, L5
 Rodríguez, M., 1998, *PhD. Thesis*, Universidad de La Laguna
 Rubin, R. H., Simpson, J. P., Haas, M. R., Erickson, E. F., 1991, *ApJ*, 374, 564 (RSHE)
 Shaw, R. A., Dufour R. J., 1995, *PASP*, 107, 896
 Wen, Z., O'Dell, C. R., 1995, *ApJ*, 438, 784